http://journal.uir.ac.id/index.php/JGEET

E-ISSN : 2541-5794
P-ISSN : 2503-216X

Journal of Geoscience,
Engineering, Environment, and Technology
Vol 11 No 3 2026

RESEARCH ARTICLE

Analysis of Earthquake Risk Zones Using the Horizontal to Vertical Spectral Ratio (HVSR) Method at Vital Objects of Radin Inten II Airport, Natar Market, and Branti Market

Muhammad Aditya [1], Nandi Haerudin[1], Nanda Hanyfa Maulida[1,*]
[1] *Geophysical Engineering, University of Lampung, Gedong Meneng, Kec. Rajabasa, Kota Bandar Lampung, Indonesia.*

*Corresponding author : nandahanyfa@eng.unila.ac.id
Tel.:+62-813-1425-2096; fax: -
Received: Oct 14, 2025; Accepted: Aug 19, 2026.
DOI: 10.24273/jgeet.2016.1.2.001

Abstract

South Lampung, Indonesia, lies within the tectonically active Indo-Australian–Eurasian subduction zone, influenced by the Lampung-Panjang and Menanga Faults. Volcanic and volcaniclastic lithologies overlying thick alluvial sediments increase seismic amplification potential. This region hosts critical infrastructure including airports and markets, but seismic hazard at these sites has not been comprehensively evaluated. Therefore, this study aims to assess seismic hazard at three critical infrastructure sites: Radin Inten II Airport, Natar Market, and Branti Market. The earthquake hazard zones were analyzed using the Horizontal to Vertical Spectral Ratio (HVSR) method, which effectively estimates site resonance frequency (f_0), amplification (A_0), and shear-wave velocity (Vs_{30}) without requiring active seismic sources or boreholes, making it ideal for rapid microzonation in urban-vital areas. Unlike previous HVSR studies in Lampung that focused on single-parameter (f_0) mapping, this study integrates five parameters (f_0, A_0, T_0, K_g, and Vs_{30}) to produce a multi-criteria hazard classification. Microtremor data were collected from 25 measurement sites using the Seismometer Rakyat Indonesia (SRI) and processed using Geopsy, Excel, and MATLAB. These analyses yielded dominant frequency (f_0) ranging from 0.6-14 Hz, amplification factor (A_0) from 0.8-5.2, dominant period (T_0) from 0.07-1.6 s, seismic vulnerability index (K_g) from 0.06-3.9 cm/s^2, and shear-wave velocity up to a depth of 30 meters (Vs_{30}) from 254-1433 m/s. These parameters were then spatially integrated to assess the seismic hazard level at each study site, with K_g and Vs_{30} as primary classifiers and f_0, A_0, T_0 as corroborating indicators. The results showed that Radin Inten II Airport and Branti Market exhibit stable seismic characteristics with high dominant frequencies (>6 Hz), low amplification (<3), short dominant periods (<0.25 s), low K_g (<1 cm/s^2), and high Vs_{30} values (>350 m/s), thus categorizing them as low-risk zones. Meanwhile, Natar Market is located within an area showing moderate dominant frequency (4-6.67 Hz) and amplification (3-6), along with a longer dominant period (0.25-0.4 s) and high Vs_{30} values (>350 m/s), placing it in a medium-risk zone. These findings provide a scientific basis for site-specific seismic risk mitigation at critical infrastructure in South Lampung.

Keywords: HVSR, dominant frequency, amplification, Vs_{30}, seismic vulnerability

1. Introduction

The Lampung region frequently experiences seismic and volcanic activity because it is located at the convergence of the Indo-Australian and Eurasian tectonic plates (Puhi et al., 2021; Sieh and Natawidjaja, 2000). The presence of the regional geological structures (Lampung–Panjang Fault and Menanga Fault) and the Indo-Australian-Eurasian subduction activity are known to increase the potential for seismic hazards in this area. The unique seismicity pattern in Lampung Province is caused by the complex interaction between the subduction zone and the Sumatra Fault System (Sieh and Natawidjaja, 2000; Widiyantoro et al., 2024). The Lampung–Panjang Fault is a NW-SE-trending normal fault that crosses the Bandar Lampung area and extends toward Lampung Bay, as confirmed by geomagnetic and DEM-based structural analysis (Sulandari et al., 2023). The Menanga Fault, oriented in a SE-W direction, traverses the Pesawaran–South Lampung corridor and passes within approximately 15-20 km of the study sites; its seismic activity was recently confirmed by the 2021 Pesawaran earthquake swarm (Nurfitriana et al., 2021). Both fault systems cross alluvial and volcanic deposits of the Lampung Formation (Mangga et al., 2010), where contrasts in subsurface impedance amplify ground shaking and increase site vulnerability during fault rupture events. This interaction creates very distinctive geological conditions, which influence the characteristics of earthquakes in the region, including their frequency, intensity, and epicenter distribution.

One significant event was the earthquake swarm that occurred in Pesawaran in January 2021. Twenty-two recurrent earthquakes were recorded with magnitudes between 1.7 and 4 and focal depths between 1 and 4 km. These events were concentrated in the Pesawaran–South Lampung area over an 11-day period. Nurfitriana et al. (2021) concluded that the Pesawaran earthquake swarm was caused by activity along the Menanga Fault, which had previously been identified only as a suspected fault.

Several studies have successfully applied HVSR for seismic hazard analysis (Amirudin et al., 2023; Prasetya et al., 2024; Putra et al., 2023; Siagian et al., 2025; Sihotang et al., 2025). Other researchers have also utilized the HVSR method for seismic hazard mapping in Lampung, though each study reveals specific limitations. Haerudin et al.

(2020) mapped disaster-prone zones across Bandar Lampung city using f_0 (dominant frequency) distribution, identifying high vulnerability areas dominated by f_0 <1.33 Hz. However, their urban-focused grid ended 25 km north of South Lampung's critical infrastructure sites, leaving airport and market facilities unassessed. Similarly, Meilinda et al. (2023) characterized low vulnerability in Padang Cermin (30 km southwest of the study area) through multi-parameter HVSR analysis, but excluded the economic hubs along Natar-Branti transport routes. Hesti et al. (2024) provided valuable soil characterization along the Menanga Fault zone in Pesawaran, documenting variable amplification in alluvium layers, but their measurements were still far from high-population markets and other critical infrastructure sites in South Lampung Regency. While these works validate HVSR methodology regionally, none specifically targeted the critical infrastructure and transport corridor in South Lampung.

Two key gaps make this study necessary. First, previous studies missed critical infrastructure sites. Radin Inten II Airport serves as the primary air transport gateway for South Lampung, while Natar Market and Branti Market are among the largest commodity distribution centers in the regency (Statistics of Lampung Selatan Regency, 2022), together representing major concentrations of economic activity and daily population exposure in the region. Furthermore, all three sites are underlain by alluvial and volcanic deposits of the Lampung Formation (Mangga et al., 2010), which are known to produce significant impedance contrasts with the underlying basement and thus have elevated amplification potential (Nakamura, 2000). However, none of these critical sites have had a formal seismic hazard assessment. Second, earlier work used limited methods. Most studies analyzed only dominant frequency (f_0) or seismic vulnerability index (K_g), while this study combines multiple parameters, namely dominant frequency (f_0), amplification factor (A_0), dominant period (T_0), vulnerability index (K_g) and shear-wave velocity up to 30 meters depth (Vs_{30}) for better hazard mapping. This study fills these gaps through a 25-point HVSR survey specifically targeting the critical infrastructure area to support South Lampung's disaster risk reduction planning.

2. Research Method

In this study, we used the Horizontal to Vertical Spectral Ratio (HVSR) method (Nakamura, 1989; Molnar et al., 2022) to evaluate the earthquake risk zone using multi-parameter analysis (dominant frequency (f_0), amplification factor (A_0), dominant period (T_0), vulnerability index (K_g), and shear-wave velocity up to 30 m depth (Vs_{30})). The research stages began with a literature review, survey design determination, and primary data acquisition in the form of microtremor data using Seismometer Rakyat Indonesia (SRI) seismograph. Signal processing followed the SESAME guidelines (SESAME, 2004) using Geopsy software (Wathelet et al., 2020). The HVSR curve at each station was computed in Geopsy as the ratio of the geometric mean of the two horizontal components and the vertical component, and the main peak of this curve was used to derive the dominant frequency (f_0) and amplification factor (A_0). Dominant period (T_0) and seismic vulnerability index (K_g) were then calculated in Microsoft Excel from f_0 and A_0. Shear-wave velocity up to 30 m depth (Vs_{30}) was obtained from 1D shear-wave velocity models derived using Monte Carlo inversion method with OpenHVSR in MATLAB (Bignardi et al., 2018) and computed using the standard Vs_{30} formula based on layer thickness and shear-wave velocity. The processed parameters were then spatially interpolated using the kriging method to generate distribution maps of f_0, A_0, T_0, K_g, and Vs_{30} across the study area. These maps were analyzed to assess the level of earthquake hazard, particularly at Radin Inten II Airport, Branti Market, and Natar Market. The complete research workflow is illustrated in Fig. 1.

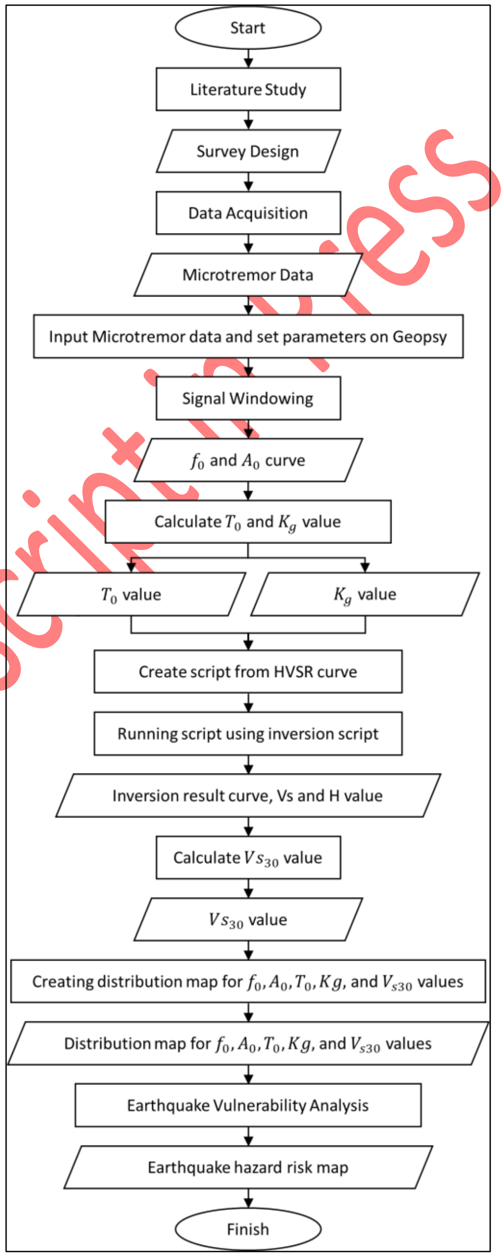

Fig. 1. Research Flowchart

2.1 Survey Design

The survey design was developed to capture the spatial variability of site-response parameters around three critical infrastructures in South Lampung, namely Radin Inten II Airport, Natar Market, and Branti Market. Measurement sites were selected to avoid obvious noise sources such as major roads, rivers, and industrial facilities, while ensuring that the main geological and geomorphological units in the study area were represented. To achieve this, the stations were arranged in an approximately uniform grid surrounding the airport and market areas, so that lateral variations in site conditions could be mapped at the scale of the wider infrastructure corridor.

A total of 25 measurement points were distributed across the study area covering approximately 60 km^2, with an average inter-station spacing of approximately 4.6 km, ranging from 2.36 to 6.5 km between neighboring sites (Table 1). This quasi-uniform configuration provides a moderate sampling density that is considered sufficient to resolve first-order spatial patterns of dominant frequency, amplification, seismic vulnerability index, and Vs_{30} across the study area. This is consistent with reconnaissance-level HVSR surveys of comparable areal extent (Koçkar and Akgün, 2008). Site selection followed standard HVSR protocols (SESAME, 2004), targeting stable geological conditions representative of local subsurface characteristics. The location of measurement points listed in Table 1 and distribution of the survey design locations can be seen in Fig. 2.

Table 1. Measurement points location and elevation

Station	Long. (°E)	Lat. (°S)	Elevation (m)
TA 1	105.159	-5.217	78
TA 2	105.100	-5.293	94
TA 3	105.098	-5.258	77
TA 4	105.102	-5.219	75
TA 5	105.157	-5.256	83
TA 6	105.174	-5.297	100
TA 7	105.171	-5.330	114
TA 8	105.212	-5.297	113
TA 9	105.210	-5.255	77
TA 10	105.213	-5.218	62
TA 11	105.257	-5.216	43
TA 12	105.251	-5.255	82
TA 13	105.250	-5.296	95
TA 14	105.299	-5.294	79
TA 15	105.304	-5.255	51
TA 16	105.307	-5.210	56
TA 21	105.360	-5.347	69
TA 24	105.185	-5.362	138
TA 25	105.207	-5.337	125
TA 26	105.236	-5.334	104
TA 27	105.276	-5.340	97
TA 28	105.311	-5.334	93
TA 29	105.353	-5.298	63
TA 31	105.350	-5.334	68
TA 32	105.323	-5.355	86

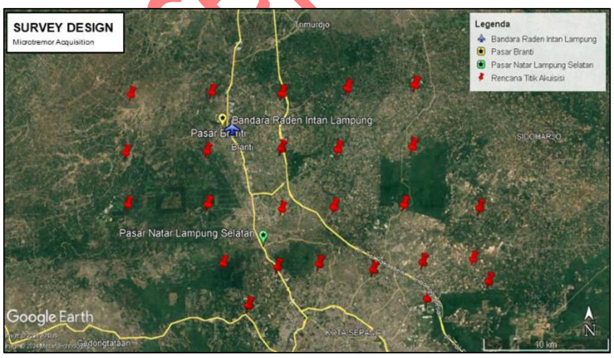

Fig. 2. Survey design for microtremor data acquisition

2.2 Microtremor Data Acquisition

Microtremor data were acquired using the Seismometer Rakyat Indonesia (SRI) at 25 measurement points, with each recording lasting 35 – 40 minutes to ensure a sufficient signal-to-noise ratio for HVSR analysis. During installation, instruments were oriented toward the north using the built-in compass and were placed on stable, flat surfaces in accordance with standard microtremor acquisition procedures (Fig. 3). GPS coordinates were recorded for precise site locations, and field notes documented local environmental conditions and potential noise sources, such as nearby traffic and human activity, so that obviously contaminated time intervals could be identified and excluded during processing. All measurements were conducted between 4 and 17 August 2024 during daytime hours (morning to late afternoon) under comparable ambient conditions, thereby minimizing systematic bias arising from temporal variability in ambient noise levels. Measurements were deliberately avoided during periods of heavy rainfall or strong wind, and all sites were situated relatively far from major roads area.

Fig. 3. Installation of the Seismometer Instrument

2.3 Data Processing

Microtremor signal processing was performed using Geopsy software (Wathelet et al., 2020) following the SESAME guidelines (SESAME, 2004). Each raw recording was first converted to a format suitable for Geopsy and visually inspected together with the field notes to identify and remove clearly noisy segments associated with transient disturbances. The remaining portions of the records were then divided into windows of 25 seconds length with no overlap, and non-stationary windows were further excluded using Geopsy's built-in anti-triggering function applied to the raw signal, with STA = 1.00 s, LTA = 30.00 s, minimum STA/LTA ratio = 0.20, and maximum STA/LTA ratio = 2.50. For each accepted window, amplitude spectra of the two horizontal components and the vertical component were computed and smoothed using the Konno–Ohmachi function (Konno and Ohmachi, 1998). The HVSR curve at each station was then obtained as the ratio of the geometric mean of the horizontal spectra to the vertical spectrum.

The dominant frequency (f_0) and amplification factor (A_0) were identified from the highest peak of the HVSR curve. Per-station uncertainty of f_0 and A_0 was automatically computed by Geopsy as the standard deviation across accepted time windows, displayed as ±1σ envelopes on each HVSR curve. Peak reliability was further assessed against the SESAME reliability and clarity criteria (SESAME, 2004), ensuring that the fundamental peak remained consistent in frequency and amplitude across windows. When multiple spectral peaks were present, the peak with the highest amplitude and most consistent shape across windows was selected as the fundamental resonance peak. An example of the output illustrating the dominant frequency value and amplification is presented in Fig. 4.

After the curve analysis, the f_0 and A_0 values for each point were exported to Microsoft Excel to calculate the dominant period (T_0) using the following equation:

$$T_0 = \frac{1}{f_0} \quad (1)$$

where T_0 is the dominant period and f_0 is the dominant frequency. And then the seismic vulnerability index (Kg) was calculated using the following equation (Nakamura, 2000):

$$K_g = \frac{A_0^2}{f_0} \quad (2)$$

where K_g is the seismic vulnerability index, A_0 is the amplification factor, and f_0 is the dominant frequency.

Shear-wave velocity profiles were derived through 1D inversion of the HVSR curves using the Monte Carlo method implemented in OpenHVSR (Bignardi et al., 2018), in which the algorithm generates a large number of random subsurface models and iteratively converges toward models whose theoretical HVSR response best fits the observed curve. This inversion approach assumes a horizontally layered, isotropic medium with no lateral velocity variation beneath each station, and treats the HVSR curve as a proxy for the ellipticity of Rayleigh waves. All model parameters, including layer thicknesses, shear-wave velocities, compressional-wave velocities, and densities were treated as free parameters within geologically plausible bounds. It should be noted that HVSR inversion is inherently non-unique; multiple subsurface models may produce equally good fits to the observed curve, and the resulting Vs_{30} estimates should therefore be interpreted as representative models rather than unique solutions. Shear-wave velocities (Vs) and layer thicknesses (H) obtained from 1D velocity models produced by OpenHVSR were used to calculate Vs_{30} value using the following equation:

$$Vs_{30} = \frac{30}{\sum_{i=1}^{N}\left(\frac{H_i}{Vs_i}\right)} \quad (3)$$

where N is the number of soil layer thicknesses, H_i is the thickness of the soil layers (m), and Vs_i is the shear-wave velocity of the soil layers. All identified parameters (f_0, A_0, T_0, Kg, and Vs_{30}) were then spatially interpolated using the kriging method to generate spatial distribution maps, which were used to delineate zones of different seismic response. The results of calculations and data processing from 25 acquisition points can be seen in Table 2.

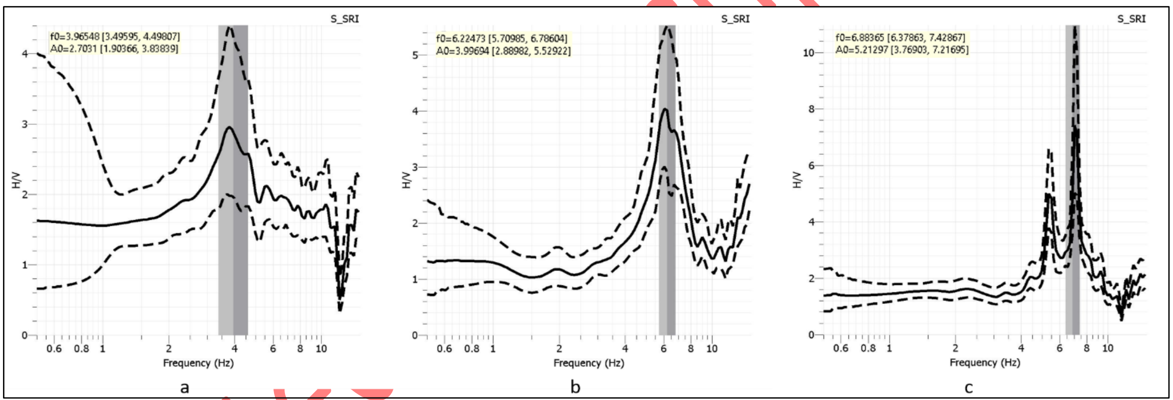

Fig. 4. Examples of HVSR processing results at (a) TA 10 station with f_0: 3.97 and A_0: 2.70, (b) TA 25 station with f_0: 6.22 and A_0: 3.99, and (c) TA 14 station with f_0: 6.88 and A_0: 5.21

Table 2. Values of f_0, A_0, T_0, Kg, and Vs_{30} at the acquisition points

No	Station	Longitude (°E)	Latitude (°S)	f_0 (Hz)	A_0	T_0 (s)	K_g (s)	Vs_{30} (m/s)
1	TA 1	105.159	-5.217	6.28	1.97	0.16	0.62	314.29
2	TA 2	105.100	-5.293	3.16	1.22	0.32	0.47	455.80
3	TA 3	105.098	-5.258	2.26	1.20	0.44	0.63	447.27
4	TA 4	105.102	-5.219	0.61	1.43	1.64	3.36	357.02
5	TA 5	105.157	-5.256	10.11	2.11	0.10	0.44	267.17
6	TA 6	105.174	-5.297	3.85	1.78	0.26	0.83	369.27
7	TA 7	105.171	-5.330	8.55	3.12	0.12	1.14	758.34
8	TA 8	105.212	-5.297	7.79	2.06	0.13	0.55	671.76
9	TA 9	105.210	-5.255	7.01	1.98	0.14	0.56	786.44
10	TA 10	105.213	-5.218	3.97	2.70	0.25	1.84	669.90
11	TA 11	105.257	-5.216	3.22	2.00	0.31	1.24	312.33
12	TA 12	105.251	-5.255	1.86	1.58	0.54	1.34	409.41
13	TA 13	105.250	-5.296	13.60	1.87	0.07	0.26	359.41
14	TA 14	105.299	-5.294	6.88	5.21	0.15	3.95	295.48
15	TA 15	105.304	-5.255	7.22	2.14	0.14	0.63	638.78
16	TA 16	105.307	-5.210	1.15	1.45	0.87	1.83	332.92
17	TA 21	105.360	-5.347	9.93	2.18	0.10	0.48	254.37
18	TA 24	105.185	-5.362	8.91	2.82	0.11	0.89	362.86

No	Station	Longitude (°E)	Latitude (°S)	f_0 (Hz)	A_0	T_0 (s)	K_g (s)	Vs_{30} (m/s)
19	TA 25	105.207	-5.337	6.22	3.99	0.16	2.57	583.01
20	TA 26	105.236	-5.334	4.52	1.57	0.22	0.54	409.05
21	TA 27	105.276	-5.340	11.84	1.04	0.08	0.09	635.18
22	TA 28	105.311	-5.334	14.03	3.20	0.07	0.73	1433.18
23	TA 29	105.353	-5.298	7.01	1.96	0.14	0.55	656.31
24	TA 31	105.350	-5.334	11.80	1.70	0.08	0.24	775.00
25	TA 32	105.323	-5.355	10.10	0.80	0.10	0.06	775.00

3. Result and Discussion

3.1 Dominant Frequency (f_0) Distribution Map

The dominant frequency (f_0) represents the natural resonance frequency of a site at which maximum seismic amplification occurs. This value reflects the thickness and impedance contrast between surface sediments and underlying bedrock (Arintalofa et al., 2020; Haerudin et al., 2020). This parameter serves as the primary indicator for subsurface stratigraphy in microtremor surveys. Lower f_0 values correspond to thicker sedimentary layers capable of substantial wave amplification, while higher f_0 values indicate thinner sedimentary layers or shallow bedrock, and therefore reduced susceptibility to seismic wave amplification (Sánchez-Sesma et al., 2011).

Across the study area, f_0 values range from 0.6-14 Hz (Fig. 5), with a mean of 6.88 Hz, a median of 7.01 Hz, and a standard deviation of ±3.84 Hz. The relatively high standard deviation reflects pronounced spatial heterogeneity in subsurface conditions, despite the study area being broadly underlain by a single formation as mapped by Mangga et al. (2010). This suggests that intra-formational variability in lithology and compaction plays a significant role in controlling local resonance characteristics.

The dominant geological unit across all measurement points is the Lampung Formation (QTl), comprising pumiceous tuff, rhyolitic tuff, compact tuff (tuffite), tuffaceous claystone, and tuffaceous sandstone (Mangga et al., 2010). This range of lithologies exhibits contrasting mechanical properties. More competent rock types such as compact tuff and tuffite tend to produce higher f_0 values because they have higher shear-wave velocities and lower compressibility. In contrast, tuffaceous claystone and tuffaceous sandstone are finer-grained and more porous, and therefore tend to yield lower f_0 values that are consistent with thicker and softer sedimentary sequences. This lithological variability within a single mapped formation explains the wide range of f_0 values observed in the study area.

Dominant frequency values were classified according to the criteria established by Kanai (as cited in Arifin et al., 2014), which correlate frequency ranges with geological characteristics and amplification potential (Fig. 5). Three frequency classifications are identified in the study area, from the low-frequency zone (f_0 < 4 Hz), the intermediate zone (4-6.67 Hz) and the high-frequency zone (6.67-14 Hz). The study area mostly lies in the high-frequency zone (red zone on the map). This is consistent with shallow volcanic bedrock exposures that might be controlled by the configuration of Pzgm (Trimulyo Marble), Kds (Sekampung Foliated Diorite), and Kgdb (Branti Granodiorite) basement units beneath the Lampung Formation (QTl) cover. These high frequencies also indicate minimal sedimentary cover and limited impedance contrast, and consequently lower seismic wave amplification potential in this zone.

Radin Inten II Airport and Branti Market are located within the high frequency zone. The high f_0 in Radin Inten II Airport is primarily driven by the Branti Granodiorite (Kgdb) intrusion. Granodioritic rocks are characterised by high shear-wave velocity and bulk density typical of crystalline igneous rocks, producing a sharp impedance contrast. Natar Market falls within the intermediate f_0 zone, where the Lampung Formation cover is estimated to be approximately 5-10 m thick. These conditions tend to enhance seismic wave amplitudes compared with adjacent hard-rock sites, especially when the incoming wave frequencies match the local resonance band. In this area, the basement units are interpreted to be at greater depth relative to the airport vicinity, with no proximal Kgdb, Kds, or Pzgm outcrops recorded. The sedimentary cover likely consists of the softer Lampung Formation members (tuffaceous claystone or tuffaceous sandstone), which generate a sufficient impedance contrast with the deeper basement to produce measurable resonance at intermediate frequencies and moderate amplification potential. Portions of the study area with f_0 below 4 Hz are interpreted as zones where the Lampung Formation attains its maximum thickness (>30 m), with the basement at considerable depth, allowing greater seismic energy to be trapped and amplified within the sedimentary column.

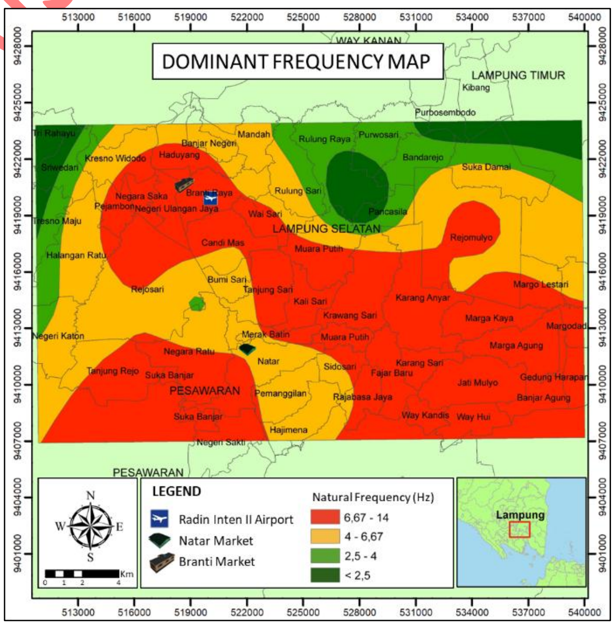

Fig. 5. Distribution map of dominant frequency (f_0) in vital areas of South Lampung Regency and its surroundings

3.2 Amplification (A_0) Distribution Map

Seismic amplification describes the increase in ground motion amplitude as seismic waves propagate through low-velocity surface sediments. In the HVSR method, the amplification factor (A_0) is derived from the peak amplitude of the H/V spectral ratio curve (Nakamura, 1989). This amplification is physically controlled by the impedance contrast between the surface layer and the underlying bedrock. When low-velocity sediments overlie high-velocity bedrock, the impedance contrast is large and the ground motion is strongly amplified. When the velocity contrast is small, the amplification is weak (Nakamura, 1989). Sites with high A_0 are more susceptible to earthquake damage, while those with low A_0 are comparatively less vulnerable. The amplification distribution map is shown in Fig. 6. The amplification values across the study area range from 0.8 to 5.2. Based on the classification of Nakamura (2000), the amplification values in the study area are classified into a low amplification zone (A_0<3) and a medium amplification zone (3 ≤A_0<6).

In Fig. 6, low amplification zone is shown in green shade and medium amplification zone in yellow shade. The spatial distribution of amplification reveals green low-amplification zones dominating the study area including Branti Airport and Branti market. These sites are underlain by shallow hard-rock or very dense soil, which produces a small impedance contrast with the underlying layers and therefore limits wave amplification. More specifically, the low A_0 values at Radin Inten II Airport are attributable to the Branti Granodiorite intrusion (Kgdb), which presents a high-velocity crystalline substrate. A similar condition applies to Branti Market, where proximity to the Pzgm and Kds basement units sustains a shallow, competent substrate with minimal velocity contrast. With shallow bedrock and low amplification these zones are expected to have low risk when an earthquake occurs. This interpretation will be strengthened in the next section.

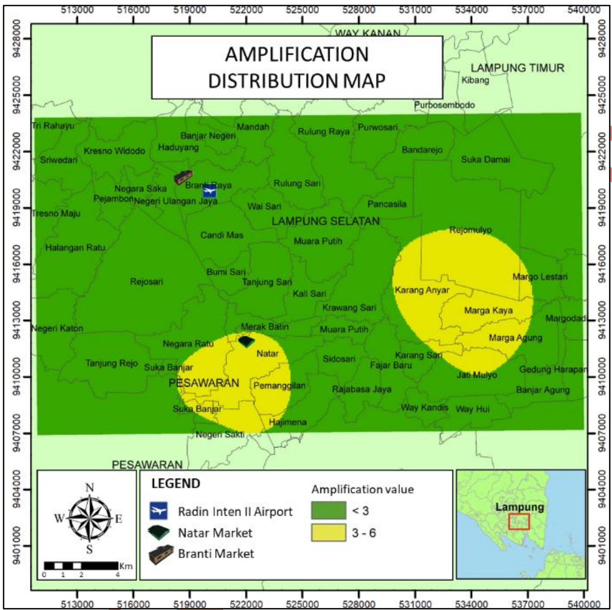

Fig. 6. Distribution map of amplification (A_0) in vital areas of South Lampung Regency and its surroundings

Some areas are clustered in yellow moderate zones, including Natar Market. Unlike the airport and Branti Market, Natar Market has no proximal Kgdb, Kds, or Pzgm outcrops in its vicinity. The surface is instead underlain by a thicker sequence of softer Lampung Formation rocks (likely tuffaceous claystone or tuffaceous sandstone), which have much lower shear-wave velocity and density than the crystalline basement. This strong contrast in properties produces a larger impedance contrast and therefore higher amplification, enhancing resonance effects and increasing the expected ground motion. These areas are expected to have higher hazard potential when an earthquake occurs. The level of the risk will be further evaluated in the subsequent hazard zonation analysis.

The A_0 values obtained in this study are broadly consistent with findings from a previous HVSR investigation conducted in Pesawaran Regency, located to the southwest and considerably distant from the present study area (Hesti et al., 2024). In that study, amplification values were predominantly below 3, corresponding to the low amplification category. Despite the considerable spatial separation between the two areas, the comparable low-to-moderate amplification range suggests that this characteristic may reflect a broader regional trend across parts of Lampung Province, with local variations controlled by the depth and lateral extent of the crystalline basement units beneath the Lampung Formation cover.

3.3 Dominant Period (T_0) Distribution Map

The dominant period (T_0) is the time required for microtremor waves to propagate through the sediment layer on the surface (Hanifah, 2023). The dominant period (T_0) is inversely related to the dominant frequency (f_0), so sites with higher f_0 values have shorter resonance periods and vice versa. Short dominant periods (T_0) are typically associated with shallow, stiff strata, while longer periods generally indicate thicker, softer sediments that can cause stronger amplification, especially for structures whose natural periods fall in the same range (e.g., Kramer, 1996; Chopra, 2012; Haghshenas et al., 2008; Bonnefoy-Claudet et al., 2006).

The distribution of dominant period values in the study area is shown in Fig. 7 and ranged from 0.07-1.6 seconds. Branti Market and the Airport have short T_0 (<0.25 s), whereas Natar Market has higher T_0 (>0.25 s). According to the soil classification based on the dominant period value by Kanai (Arifin et al., 2014) the T_0 value can be divided into four classifications. The period of 0.05-0.15 is Type I (dark green zone), 0.15-0.25 is type II (light green zone), 0.25 – 0.40 is type III (orange zone) and the period > 0.40 is type IV (red zone).

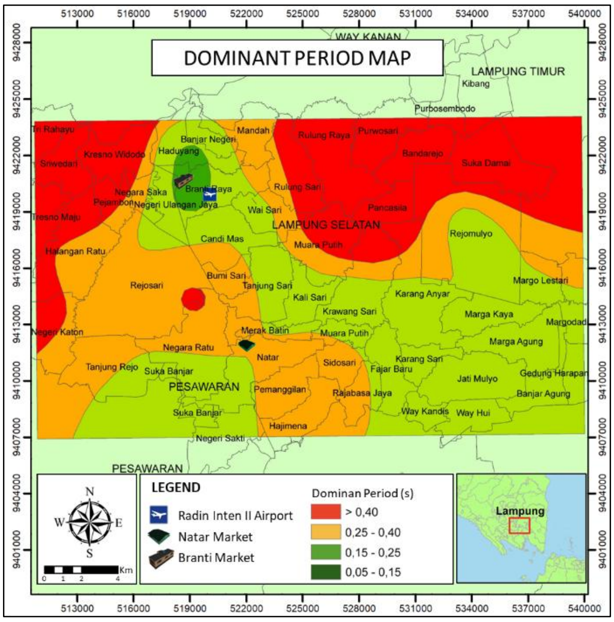

Fig. 7. Distribution map of dominant period (T_0) in vital areas of South Lampung Regency and its surroundings

Branti Market is classified as Type I, characterised by hard soil conditions. This is consistent with the proximity of the Pzgm and Kds basement units in this sector, where shallow crystalline bedrock (marble, schist, and foliated diorite) produces the stiff, low-period response typical of hard ground. Radin Inten II Airport is classified as Type II, indicating medium soil conditions that match the thin tuffaceous cover of the Lampung Formation (QTl). The nearby Branti Granodiorite intrusion (Kgdb), which crops out south of the airport, likely makes the subsurface stiffer in this area, reduces the effective sediment thickness, and helps maintain the relatively short T_0 values. Natar Market is classified as Type III, indicating soft soil conditions consistent with a thicker sequence of the softer Lampung Formation rocks overlying a deeper basement, as previously discussed in the f_0 and A_0 analyses.

The T_0 pattern is consistent with the f_0 results, where Radin Inten II Airport and Branti Market, which show short T_0 and high f_0, correspond to stiff sites with limited amplification potential. In contrast, the longer T_0 values at Natar Market reflect softer, thicker alluvial deposits, in agreement with its higher A_0. This indicates that all three sites' dynamic responses to earthquake loading differ from each other, and Natar may experience more significant shaking for earthquakes whose predominant periods match the 0.25–0.40 s range.

From an engineering perspective, the T_0 ranges at each site have direct implications for building vulnerability. The natural period of a building can be approximated as $T_{\text{structure}} \approx 0.1 \times N$, where N is the number of storeys (Chopra, 2012). At Natar Market, the new two-storey reinforced-concrete market building has an estimated structural period of about 0.2 s. This value is slightly lower than the site period range of 0.25-0.40 s, but the two ranges are close enough to suggest a partial resonance risk: strong ground motions with dominant periods around 0.25-0.30 s could excite the building more strongly than if it were founded on stiffer ground.

At Radin Inten II Airport, the building complex includes multi-storey reinforced-concrete structures, such as a four-storey car park and a large terminal, with estimated structural periods of roughly 0.3-0.4 s. The measured site period at the airport (0.15-0.25 s, Type II) is shorter than these values, so the potential for strong soil–structure resonance is lower under typical shaking. However, long-span terminal components with lower natural frequencies should still be considered in detailed seismic design.

Branti Market is dominated by single- to two-storey traditional buildings with estimated periods of 0.1-0.2 s. This range overlaps with the Type I site period band (<0.15 s), indicating a low but non-zero resonance potential. Overall, the three sites are expected to respond differently to earthquake loading, with Natar Market being more exposed to resonance effects for earthquakes whose predominant periods fall within the 0.25-0.40 s range, which has implications for both occupant safety and the structural performance of the market building.

3.4 Seismic Vulnerability Index (K_g) Distribution Map

The seismic vulnerability index (K_g) describes how strongly an area is expected to be affected by earthquakes based on its subsurface conditions. It represents the susceptibility of the soil to deformation caused by seismic loading. The K_g value is calculated from the dominant frequency (f_0) and the amplification factor (A_0). The K_g value is proportional to the amplification factor and inversely proportional to the dominant frequency. Nakamura (2000) noted that K_g values exceeding 20 are characteristic of sites where ground deformation is substantial, while very small K_g values are associated with sites that sustain little to no damage. The distribution of K_g values in the study area is shown in Fig. 8. The K_g values obtained in this study range from 0.06-3.9 cm/s². All values fall well below the threshold of 20 suggested by Nakamura (2000), indicating that the study area as a whole is characterised by low to moderate susceptibility to seismic ground deformation.

Radin Inten II Airport and Branti Market are situated within lower vulnerability zones (K_g<1), consistent with the Branti Granodiorite (Kgdb) cropping out in the vicinity of the airport and the Pzgm and Kds units underlying Branti Market. This lithology produces high f_0 values and low A_0, jointly suppressing K_g to its minimum range. The low K_g at these sites implies that under seismic loading, the ground is expected to undergo minimal deformation. Structures founded on such competent substrates are at comparatively lower risk of earthquake-induced ground failure.

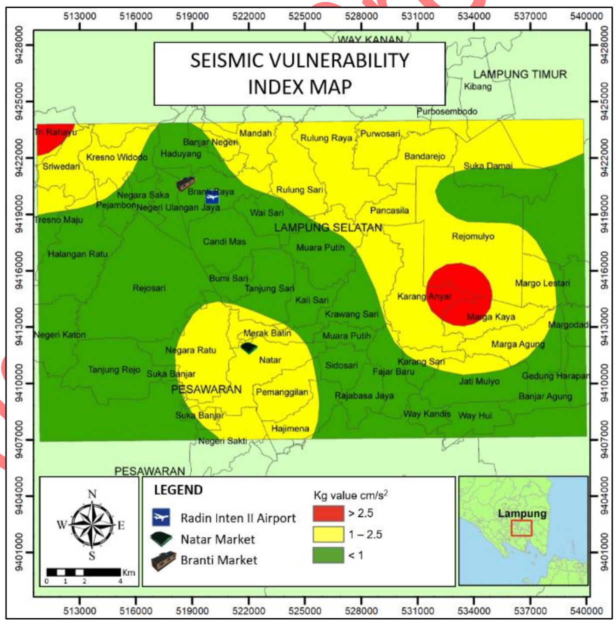

Fig. 8. Distribution map of seismic vulnerability index (K_g) in vital areas of South Lampung Regency and its surroundings

Natar Market is located in an area of relatively higher K_g values within the study area (1<K_g<2.5). Although the absolute K_g values at Natar Market are still low with respect to Nakamura's (2000) damage threshold, they are higher than those at the airport and Branti Market. This relative increase indicates that Natar is more susceptible to ground deformation. In practice, this may appear as stronger amplified shaking, which could affect the structural performance of the two-storey market building during a significant earthquake. A few small regions such as parts of Karang Anyar, Rejomulyo, Marga Kaya, and a portion of Tri Rahayu exhibit the highest K_g values in the study area (K_g>2.5). This is probably where the softest and thickest Lampung Formation units, such as tuffaceous claystone or tuffaceous sandstone, occur without nearby competent basement rock. Despite remaining within the low-to-moderate range, these areas should be given priority in detailed mitigation planning.

The K_g values obtained in this study are notably lower than those reported from comparable HVSR investigations in Lampung Province. A microseismic study at the ITERA campus in South Lampung Regency, which is also underlain by the Lampung Formation (QTl), reported K_g values between 2 and 15, with the northern campus classified as having moderate to high vulnerability (Salsabila et al., 2025). In contrast, the K_g range in this study is much lower (0.06-3.9 cm/s^2), mainly because crystalline basement units (Kgdb, Pzgm, Kds) are present within the area and act to limit both amplification and dominant period. This produces a more favourable subsurface condition than in areas that are underlain only by the Lampung Formation. The K_g pattern also matches the distributions of f_0, A_0, and T_0, indicating that the main critical infrastructure sites are located on relatively stable ground, while the surrounding patches with moderate to high K_g should receive higher priority in mitigation planning.

3.5 Shear-Wave Velocity (Vs_{30}) Distribution Map

The subsurface soil and rock conditions significantly affect earthquake-induced ground motion; therefore, Vs_{30} (average shear-wave velocity up to 30 meters) is widely used as a key physical parameter to classify site conditions (BSN, 2019; Boore et al., 2011). The upper 30 m of the subsurface plays a dominant role in controlling seismic wave amplification (Boore et al., 2011). Softer soils tend to produce stronger shaking compared to hard or dense rock formations. The distribution map of Vs_{30} values is shown in Fig. 9.

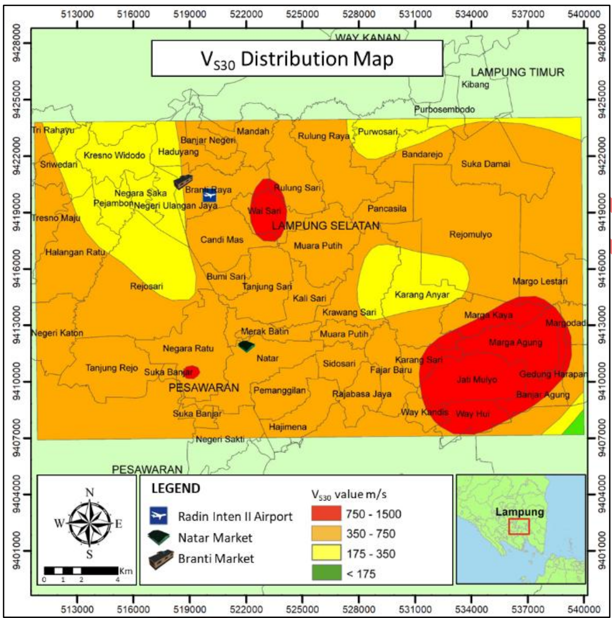

Fig. 9. Distribution map of Vs_{30} values in vital areas of South Lampung Regency and its surroundings

The Vs_{30} values obtained in this study range from 254 to 1433 m/s. Based on the Indonesian National Standard SNI 1726:2019 (BSN, 2019), the values correspond to four site classifications, SB, SC, SD and SE. SB represents rock sites with Vs_{30} between 750–1500 m/s. SC represents very dense soil and soft rock with Vs_{30} between 350–750 m/s. SD represents stiff soil with Vs_{30} between 175–350 m/s. SE represents soft soil with Vs_{30} values below 175 m/s. In the Vs_{30} map, areas with high Vs_{30} values (SB) are shown in red, moderate Vs_{30} (SC) in orange, low Vs_{30} (SD) in yellow, and very low Vs_{30} (SE) in green.

All vital sites studied are located within SC zones, although Branti Market lies near the lower bound of this class, approaching the SC–SD boundary. SC zones indicate hard to very dense soils and soft rock types that generally provide better resistance to strong shaking than those in SD–SE classes. This SC-class dominance is geologically consistent with the preceding analyses, where the crystalline basement units (Kgdb, Pzgm, Kds) lie beneath the study area below the Lampung Formation (QTl). Around Radin Inten II Airport and Branti Market, these basement rocks are exposed or occur at shallow depth. Their presence produces the high Vs_{30} values that are typical of competent igneous and metamorphic rocks. This result is further supported by Rustadi and Rananda (2020), who reported that the Lampung Formation and Muda Volcanic Formation in the Bandar Lampung area are classified as site class C with $Vs_{30} > 360$ m/s, consistent with the SC-class results obtained in the present study.

The western vicinity of Branti Market is located near the SC–SD boundary, with Vs_{30} values in the low to moderate range, suggesting that small variations in local geology could still influence the level of amplification there. This is somewhat unexpected because nearby Kds and Pzgm outcrops would normally be associated with higher Vs_{30}. Several factors could explain this, such as weathering of the upper rock surface, interbedding of softer Lampung Formation units, or averaging effects over the 30 m depth used to compute Vs_{30}. However, without additional geotechnical or geophysical data, the exact cause remains unclear and should be investigated further. The SC-to-SD transition observed in surrounding areas reflects zones where the basement lies at greater depth beneath a thicker Lampung Formation cover.

It should be noted that Vs_{30} values derived from HVSR-based inversion carry greater uncertainty compared with direct geophysical measurements such as MASW (Multichannel Analysis of Surface Waves) or borehole seismic surveys. The HVSR inversion relies on a 1-D layered model assumption and is non-unique. Moreover, the inverted Vs_{30} may be influenced by ambient noise directionality and lateral subsurface heterogeneity. However, the consistency between Vs_{30} results and the other HVSR parameters (f_0, A_0, K_g) across all sites provides a reasonable basis for the site classification presented here. The agreement with the geological-based classification by Rustadi and Rananda (2020) for the same geological formations further supports the reliability of the results. Future investigations should include MASW or seismic refraction measurements for direct validation. Overall, the predominance of SC conditions at Radin Inten II Airport, Natar Market, and Branti Market supports the earlier interpretation from f_0, T_0, A_0, and K_g that these critical infrastructures are located on relatively stable ground, even though surrounding SD–SE patches may experience stronger amplification during large earthquakes.

3.6 Earthquake Hazard Zonation Analysis

As a synthesis of the seismic parameters, the earthquake hazard risk map for vital areas in South Lampung Regency and its surroundings is shown in Fig. 10. The map was produced by combining five seismic parameters (f_0, A_0, T_0, K_g, and Vs_{30}). Each measurement point was assigned a score based on these parameter values. Vs_{30} and K_g were treated as the primary classifiers, where high Vs_{30} and low K_g indicate low hazard, and low Vs_{30} combined with high K_g indicate high hazard. The parameters f_0, A_0, and T_0 were used as supporting constraints. A_0 represents the magnitude of ground motion amplification. The parameters f_0 and T_0 help to interpret subsurface conditions and to evaluate the potential for resonance between the site period and the natural period of typical local structures. Points where T_0 falls within the expected structural period range (about 0.2–0.4 s) were assigned higher hazard scores because of this resonance potential. The scoring results were then spatially interpolated to produce continuous hazard zones, classified into three categories: low, medium, and high.

The classification thresholds applied are as follows. Low hazard zones are characterised by high to moderate Vs_{30} (SC or better), low K_g, low to moderate A_0, and T_0 that does not closely match the natural period of dominant local structures. Moderate hazard zones are characterised by moderate Vs^{30} (SC–SD), moderate K_g, moderate to slightly elevated A_0, and T_0 in the range of 0.2–0.4 s where partial resonance with typical structures is possible. High hazard zones are characterised by the lowest Vs_{30} (SD–SE), the highest K_g values in the study area, high A_0, and T_0 relevant to the period of common 1–2 storey buildings in the surrounding area.

The high-risk zone (red) forms a concentrated elliptical-shaped area centered around Karang Anyar, extending slightly northeast toward Rejomulyo, Marga Kaya and southeast toward Krawang Sari. These locations exhibit comparatively higher K_g and lower Vs_{30}, implying softer soils and greater potential for amplified shaking, so they should be prioritized for mitigation measures such as structural strengthening and planning of evacuation routes. Surrounding the high-risk core, the moderate risk zone (yellow) appears with large areal coverage on the map.

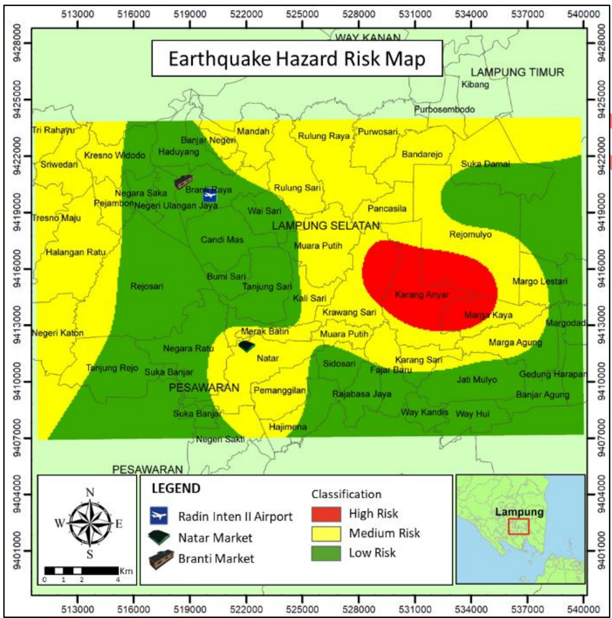

Fig. 10. Earthquake hazard risk map for vital areas of South Lampung Regency and its surroundings

These zones stretch northeastward through Pancasila, Rejomulyo, Purwosari, and Bandarejo, westward through Tanjung Sari, Kali Sari, Muara Putih, and Wai Sari and southward into Natar (including Natar Market), Sidosari, Fajar Baru, Rajabasa Jaya, and Hajimena. A moderate risk zone also appears in the western part of the map which is part of Pesawaran Regency. These locations exhibit moderate K_g values and SC–SD site classes suggest thinner sediments and lower site response than in the high-risk areas.

Low-risk zones (green) are distributed across the western and southern parts of the study area surrounding the medium-risk zone. These zones are located mainly along the administrative boundaries between South Lampung, Pesawaran, and Bandar Lampung. Radin Inten II Airport and Branti Market fall entirely within these low-risk zones. These areas are characterized by low seismic vulnerability index (K_g) values and relatively high Vs_{30}, indicating hard to very dense ground or shallow bedrock with a small impedance contrast to underlying layers, which limits local site amplification.

The spatial pattern of the hazard zones is qualitatively consistent with the regional geological framework. Low-risk zones coincide with areas where the crystalline basement units (Kgdb, Pzgm, Kds) are exposed or occur at shallow depth, producing competent ground conditions. High and moderate-risk zones correspond to areas underlain by thicker and softer Lampung Formation members, where greater sediment thickness and lower Vs_{30} promote stronger amplification. This geological consistency provides qualitative support for the hazard zonation, although a formal quantitative validation against independent hazard maps or historical earthquake damage records was not conducted in this study.

Based on the map, the three vital objects sit in different risk zones. Radin Inten II Airport and Branti Market are both located in the green (low risk) zone, meaning they are relatively safe from severe earthquake shaking. These two locations can potentially serve as emergency hubs for evacuation, logistics distribution, and relief operations during a disaster. Natar Market, however, falls within the yellow (moderate risk) zone. This busy market area is likely crowded with people and dense with structures, making it a priority location for mitigation efforts such as building inspections, structural reinforcement, and public earthquake awareness programs. This study, however, evaluates local site effects only and does not provide a full seismic risk assessment. A comprehensive risk study would also need source hazard characterization, structural vulnerability analysis, and exposure data. Within the more limited scope of site-effect analysis, the ground conditions at these two locations are favorable and could support their use as emergency hubs for evacuation, logistics, and relief operations, provided that the structural performance of the existing buildings is confirmed through dedicated engineering evaluations.

Beyond immediate disaster response, these risk zone results can also directly inform local spatial planning policies. Authorities should consider restricting high-density development in the red and yellow zones to reduce future exposure. Earthquake-resistant building codes need to be enforced in moderate-risk areas, particularly around Natar Market where public activity is high. The low-risk green zones, including the areas around the airport and Branti Market, should be designated as strategic locations for emergency facilities and post-disaster infrastructure recovery. But the structural assessments must be provided to confirm the suitability of existing buildings. In this way, the hazard map serves not only as a warning tool but also as a practical guide for long-term land use planning and community resilience building.

4. Conclusion

Microtremor analysis using the Horizontal to Vertical Spectral Ratio (HVSR) method reveals that subsurface conditions across the study area are characterized by significant spatial variability in all five measured parameters. These include dominant frequency (f_0) ranging from 0.6 to 14 Hz, amplification factor (A_0) from 0.8 to 5.2, dominant period (T_0) from 0.07 to 1.6 s, seismic vulnerability index (K_g) from 0.06 to 3.9 cm/s², and shear-wave velocity (Vs_{30}) from 254 to 1433 m/s. This variability occurs despite the study area being broadly underlain by a single geological formation, confirming that intra-formational lithological contrasts and the depth to crystalline basement units are the primary controls on local site response. The multi-parameter integration approach adopted in this study provides a more comprehensive hazard characterisation than single-parameter analyses previously conducted in the Lampung region.

Radin Inten II Airport and Branti Market are classified as low-risk zones, characterized by high f_0 (>6 Hz), low A_0 (<3), short T_0 (<0.25 s), low K_g (<1 cm/s²), and Vs_{30} between 350-750 m/s. All values consistently indicate shallow, stiff ground with minimal seismic amplification potential supported by the presence of shallow crystalline basement units (Kgdb, Pzgm, and Kds) shown in the geological map, suggesting that both sites are relatively stable under seismic loading within the limitations of a site-effect study. Natar Market is classified as a moderate-risk zone, where f_0 ranges from 4-6.67 Hz, medium A_0 (3-6), medium T_0 (0.25-0.40 s), moderate K_g values and Vs_{30} between 350750 m/s, reflect thicker sediment layers of the Lampung Formation with greater susceptibility to ground shaking. The high-risk zone centered around Karang Anyar shows the most unfavorable combination of parameters, with comparatively lower Vs_{30}, higher K_g, and higher A_0 (although the f_0 is high and T_0 is low), making it the most vulnerable area in the study region. The relatively high f_0 at some stations in this zone is not necessarily indicative of stiff ground conditions. Rather, it reflects a thin but highly contrasting soft layer above a deeper impedance boundary. In this case, K_g and Vs_{30} are more reliable vulnerability indicators than f_0 alone.

These findings carry direct implications for seismic risk mitigation and spatial planning in South Lampung. Structures in the moderate-risk zone around Natar Market should be designed to withstand ground motions with predominant periods of 0.25-0.40 s, and existing buildings in this area warrant structural inspection and, where necessary, retrofitting. The high-risk zone around Karang Anyar requires prioritization in local disaster risk reduction planning, including structural vulnerability assessment and enforcement of seismic-resistant building codes. Radin Inten II Airport and Branti Market, situated on stable, low-risk ground, are geotechnically suitable candidates for designation as emergency response and post-disaster logistics hubs, provided that the structural performance of existing buildings is confirmed through dedicated engineering evaluations. For Radin Inten II Airport specifically, the low-risk ground conditions provide a favourable baseline for continued safe operation. However, periodic structural monitoring of the terminal and runway infrastructure remains advisable given the region's active tectonic setting. It should also be noted that the reconnaissance-level spatial resolution of 25 measurement points limits the precision of hazard zone boundaries. Additionally, Vs_{30} estimation is derived indirectly from HVSR inversion rather than from direct borehole or active-source measurements. Future work should incorporate denser measurement networks, direct geotechnical validation (e.g., MASW or borehole surveys), and integration with probabilistic seismic hazard assessment (PSHA) to provide a more complete risk picture for the region.

Acknowledgement

The authors would like to express sincere gratitude to the Geophysical Engineering Laboratory, University of Lampung, for providing access to the Seismometer Rakyat Indonesia (SRI) instruments used in this study. The authors also thank all field assistants who supported microtremor data acquisition at Radin Inten II Airport, Natar Market, and Branti Market. This research was funded by the Non-Tax State Revenue (PNBP) through the DIPA BLU Universitas Lampung Fiscal Year 2024 under the Professorship Research Scheme (Skema Penelitian Profesorship).

References

Amirudin, A., Prasetyo, A.R., Faris, F., 2023. Seismic vulnerability analysis using the horizontal to vertical spectral ratio method on the West Palu Bay coastline. Journal of Geoscience, Engineering, Environment, and Technology, 8(02-2), 121–130. https://doi.org/10.25299/jgeet.2023.8.02-2.13879

Arifin, S.S., Mulyatno, B.S., Marjiyono, Setianegara, R., 2014. Penentuan zona rawan guncangan bencana gempa bumi berdasarkan analisis nilai amplifikasi HVSR mikrotremor dan analisis periode dominan daerah Liwa dan sekitarnya. JGE (Jurnal Geofisika Eksplorasi), 2(1), 30–40.

Arintalofa, V., Yulianto, G., Harmoko, U., 2020. Analisa mikrotremor menggunakan metode HVSR untuk mengetahui karakteristik bawah permukaan manifestasi panas bumi Diwak dan Derekan berdasarkan nilai Vp. Jurnal Energi Baru dan Terbarukan, 1(2), 54–61.

BSN, 2019. SNI 1726:2019 - Tata cara perencanaan ketahanan gempa untuk struktur bangunan gedung dan nongedung. Badan Standardisasi Nasional, Jakarta.

Bignardi, S., Yezzi, A.J., Fiussello, S., Comelli, A., 2018. OpenHVSR - Processing toolkit: enhanced HVSR processing of distributed microtremor measurements and spatial variation of their informative content. Computers & Geosciences, 120, 10–20. https://doi.org/10.1016/j.cageo.2018.07.006

Boore, D.M., Thompson, E.M., Cadet, H., 2011. Regional correlations of VS30 and velocities averaged over depths less than and greater than 30 meters. Bulletin of the Seismological Society of America, 101(6), 3046–3059. https://doi.org/10.1785/0120110071

Bonnefoy-Claudet, S., Cotton, F., Bard, P.-Y., 2006. The nature of noise wavefield and its applications for site effects studies: a literature review. Earth-Science Reviews, 79(3-4), 205–227.

Chopra, A.K., 2012. Dynamics of structures: theory and applications to earthquake engineering. 4th ed. Prentice Hall, Upper Saddle River, NJ.

Haerudin, N., Alami, F., Yogi, I.B.S., 2020. The effect site analysis based on microtremor data using the Horizontal to Vertical Spectral Ratio (HVSR) method in the Bandar Lampung City. Journal of Physics: Conference Series, 1572(1), 012075. https://doi.org/10.1088/1742-6596/1572/1/012075

Haghshenas, E., Bard, P.-Y., Theodulidis, N., 2008. Empirical evaluation of microtremor H/V spectral ratio. Bulletin of Earthquake Engineering, 6(1), 75–108.

Hanifah, D.R., 2023. Penyusunan peta kerentanan gempa di Berbah Kabupaten Sleman menggunakan metode Horizontal to Vertical Spectral Ratio (HVSR) berdasarkan pengukuran mikrotremor di lapangan. Undergraduate thesis. Universitas Islam Indonesia, Yogyakarta. Available at: https://dspace.uii.ac.id/handle/123456789/42791 (Accessed 12 November 2025).

Hesti, H., Mulyasari, R., Hidayatika, A., Haerudin, N., Nurlaili, J., 2024. Analisis karakteristik lapisan tanah di daerah patahan lokal berdasarkan data mikrotremor di Kabupaten Pesawaran. Journal Online of Physics, 9(3), 136–141.

Koçkar, M.K., Akgün, M., 2008. On the use of microtremor recordings in the determination of local site effects. Bulletin of Earthquake Engineering, 6(4), 447–468.

Kramer, S.L., 1996. Geotechnical earthquake engineering. Prentice Hall, Upper Saddle River, NJ.

Mangga, S.A., Amirudin, Suwarna, N., Gafoer, S., Sidarto, 2010. Geological map of the Tanjungkarang quadrangle, Sumatera. Pusat Survei Geologi, Bandung.

Meilinda, A., Suryani, I., Putra, J.A., 2023. Analisa potensi kerentanan tanah daerah Padang Cermin menggunakan metode Horizontal to Vertical Spectral Rasio. Jurnal Lingkungan dan Bencana Geologi, 14(2), 76–84.

Molnar, S., Cassidy, J.F., Castellaro, S., Cornou, C., Crow, H., Hunter, J.A., Philips, D., Roten, D., Thompson, E.M., 2022. Review of the horizontal-to-vertical spectral ratio (HVSR) method. Surveys in Geophysics, 43, 431–474.

Nakamura, Y., 1989. A method for dynamic characteristics estimation of subsurface using microtremor on the ground surface. Quarterly Report of the Railway Technical Research Institute, 30(1), 25–33.

Nakamura, Y., 2000. Clear identification of fundamental idea of Nakamura's technique and its applications. In: Proceedings of the 12th World Conference on Earthquake Engineering, Auckland, paper 2656.

Nurfitriana, I., Wibowo, A., Rudianto, R., 2021. Relokasi gempa bumi swarm di Pesawaran-Lampung, Januari 2021. Jurnal Geocelebes, 5(1), 91–101.

Prasetya, A.R., Faris, F., Rahardjo, A.P., 2024. Study of local site effects for seismic vulnerability mitigation based on microtremor measurements in the NYIA airport area. GEOMATE Journal, 26(113), 148–155.

Puhi, A.R., Widiyantoro, S., Gunawan, H., Nugraha, A.D., 2021. Crustal structure study in Lampung region using teleseismic receiver function analysis. Journal of Physics: Conference Series, 2110, 012002.

Putra, A.K., Yatini, Y., Paripurno, E.T., 2023. Application of HVSR method on microtremor data for analysis of earthquake potential in Candipuro District, Lumajang, Indonesia. Journal of Geoscience, Engineering, Environment, and Technology, 8(4), 288–294.

Rustadi, R., Rananda, E., 2020. Rock formation and site class in Bandar Lampung. JGE (Jurnal Geofisika Eksplorasi), 6(3), 183–189. https://doi.org/10.23960/jge.v6i3.101

Sánchez-Sesma, F.J., Rodríguez, M., Iturrarán-Viveros, U., Luzón, F., Campillo, M., Margerin, L., García-Jerez, A., Suárez, M., Santoyo, M.A., Ordaz, M., 2011. A theory for microtremor H/V spectral ratio: application for a layered medium. Geophysical Journal International, 186(1), 221–225.

Salsabila, R.S., Fattah, E.I., Darisma, D., Hidayati, D.M., Hasanah, U., 2025. Mikrozonasi seismik menggunakan metode Horizontal to Vertical Spectral Ratio (HVSR) di Kampus ITERA, Lampung Selatan. INSOLOGI (Jurnal Sains dan Teknologi), 4(5), 1196–1202.

SESAME, 2004. Guidelines for the implementation of the H/V spectral ratio (HVSR) technique on ambient vibrations: measurements, processing and interpretation. Deliverable D23.12, European Commission, Research General Directorate, Brussels.

Siagian, S., Refrizon, Hadi, A.I., 2025. Mapping of natural frequency, amplification, seismic vulnerability, and Vs30 velocity in Selebar District, Bengkulu City. Jurnal Fisika Universitas Negeri Semarang, 15(1), 20–29.

Sieh, K., Natawidjaja, D.H., 2000. Neotectonics of the Sumatran fault, Indonesia. Journal of Geophysical Research: Solid Earth, 105(B12), 28295–28326.

Sihotang, N., Refrizon, Hadi, A.I., 2025. Resonance and damping ratio analysis of the Baiturrahman Mosque Tower based on earthquake ground shaking. Journal of Geoscience, Engineering, Environment, and Technology, 10(2), 270–274.

Statistics of Lampung Selatan Regency, 2022. Lampung Selatan Regency in figures 2022. BPS-Statistics of Lampung Selatan Regency, Kalianda.

Sulandari, S., Nurfitriana, I., Hesti, H., Rudianto, R., 2023. Deliniasi struktur Sesar Lampung-Panjang dan identifikasi kelurusan struktur bawah permukaan di Bandar Lampung dan sekitarnya menggunakan metode magnet. Jurnal Geologi dan Sumberdaya Mineral, 24(3), 145–158.

Wathelet, M., Chatelain, J.-L., Cornou, C., Di Giulio, G., Guillier, B., Ohrnberger, M., Savvaidis, A., 2020. Geopsy: a user-friendly open-source tool set for ambient vibration processing. Seismological Research Letters, 91(3), 1878–1889.

Widiyantoro, S., Gunawan, H., Nugraha, A.D., Taufiqurrahman, I., Widodo, I., 2024. Seismicity of Sumatra and western Sunda Arc and implications for back-arc thrusting. Scientific Reports, 14, 13115.